Phytopathology Research

RESEARCH

Open Access

Pathogenic function of the natural variation of CP in WYMV and CWMV

Jiajia Lei[1,2], Shuang Liu[1,2], Zhuangxin Ye[1,2], Zhiqing Chen[1,2], Hanhong Liu[3], Kaili Zhong[1,2], Qisen Lu[1,2], Juan Zhang[1,2], Jianping Chen[1,2], Jian Yang[1,2*] and Peng Liu[1,2*]

Abstract

The soil-borne viral disease, caused by wheat yellow mosaic virus (WYMV) and Chinese wheat mosaic virus (CWMV), is one of the most destructive wheat diseases in China. Considering the large wheat growing area in China, the genetic diversity of WYMV and CWMV could be high in the country. However, studies on genetic diversity of WYMV and CWMV in China are limited, making it difficult to prevent and control viral diseases on wheat. During 2021–2022, the wheat leaves with typical yellow mosaic virus symptoms were randomly collected from wheat fields in seven provinces. Nine WYMV and one CWMV isolates were identified in the samples using small RNA sequencing and RACE technology. Sequence alignment showed that several amino acid substitutions were occurred in the coat protein (CP) from these isolates. Moreover, we replaced the CP of WYMV and CWMV infectious clones with CP of newly identified isolates and found that natural variation of CP is involved in the pathogenicity of WYMV. Moreover, the WYMV infectious clones containing CP of the WYMV isolates from Junan at Shandong Province or Yangzhou at Jiangsu Province have enhanced WYMV infection in several local wheat resistance cultivars. Taken together, our findings suggest that the distribution of WYMV and CWMV in wheat growing areas has expanded in these years and the natural variation of viral genome is involved in pathogenicity of WYMV. Our results also provide a theoretical basis to explain the real distribution of wheat viral resistance varieties in China.

Keywords Wheat, WYMV, CWMV, Pathogenicity, Coat protein

Background

Soil-borne wheat viruses are important pathogens of wheat (*Triticum aestivum*), that cause severe damage to wheat crops, including wheat yellow mosaic virus (WYMV) and Chinese wheat mosaic virus (CWMV) in Asia (Sawada 1972; Diao et al. 1999), wheat spindle streak mosaic virus (WSSMV) in Europe and North America (Sohn et al. 1994), soil-borne wheat mosaic virus (SBWMV) in the United States (McKinney 1923; Shirako et al. 2000), and soil-borne cereal mosaic virus (SBCMV) in Europe (Kanyuka et al. 2003). In China, the prevalence of CWMV and WYMV disease causes grain yield loss by 10–30% and sometimes up to 70% in severe cases (Chen 2010). These viruses are transmitted by the zoospores of the plasmodiophoraceous root parasite *Polymyxa graminis* (Shirako et al. 2000). Due to the long-term survival of dormant spores of *P. graminis*, the viral diseases are difficult to eliminate using conventional crop management or chemical control methods (Adams 2007). Breeding wheat varieties with stable and durable disease

*Correspondence:
Jian Yang
nather2008@163.com
Peng Liu
wood319@126.com
[1] State Key Laboratory for Managing Biotic and Chemical Threats to the Quality and Safety of Agro-Products, Institute of Plant Virology, Ningbo University, Ningbo 315211, China
[2] Key Laboratory of Biotechnology in Plant Protection of MARA and Zhejiang Province, Institute of Plant Virology, Ningbo University, Ningbo 315211, China
[3] Junan County Bureau of Agriculture and Country, Linyi 276600, China

resistance in field is the most effective way to control the disease (Chen et al. 2014).

Since the 1960s, soil-borne wheat yellow mosaic disease caused by WYMV has been reported in various regions of China. In Shandong Province, this viral disease was first identified in 1958 and then began to expand with the emergence of highly susceptible varieties in the coastal areas of Shandong Province in the 1970s. This incidence also occurred in Hubei Province, wherein mosaic disease was identified in the 1960s, and the severity of viral disease gradually increased in the 1970s, especially in some areas of northeastern Hubei, which accounted for 4% of the total sown area of wheat. In Shaanxi Province, a mosaic disease caused by WYMV was discovered in Zhouzhi County in 1974, which gradually spread to the Guanzhong Plain. In Zhejiang and Jiangsu provinces, mosaic disease was recorded in the 1960s, causing severe damage to wheat crops. Mosaic diseases caused by WYMV have been reported in more regions of China, especially in the middle and lower reaches of the Yangtze River, Huaihe River Basin, and Weihe River Basin (Han et al. 2000; Chen 2010). In the 1990s, the CWMV was first described in China. Since then, a new trend of westward and northward expansion of CWMV has been observed in severely infected areas in China. Moreover, co-infection with CWMV and WYMV has also been identified in several wheat-producing regions of China, resulting in much severer symptoms in the field (Diao et al. 1999).

WYMV along with WSSMV belong to the genus *Bymovirus,* while CWMV is a member of the genus *Furovirus* (family *Virgaviridae*) (Yang et al. 2022). In Japan, WYMV is classified into three pathotypes (I–III) based on its pathogenicity in wheat cultivars. Pathotype I causes systemic infection in the cultivars Nambukomugi and Fukuhokomugi, but not in the cultivar Hokkai 240; pathotype II causes a systemic infection only in Nambukomugi; pathotype III causes infection in all three wheat cultivars (Ohki et al. 2014; Ohki et al. 2019). In China, the phylogenetic relationships of WYMV isolates are congruent with their locations, suggesting an origin-dependent population genetic structure (Sun et al. 2013a).

WYMV has flexuous filaments with two modal lengths of approximately 550 and 275 nm, which contain a bipartite single-strand positive RNA (Ohki et al. 2019) and encode a total of 11 proteins (Chung et al. 2008). Meanwhile, CWMV has a bipartite single-strand positive RNA genome that encodes seven proteins (Diao et al. 1999; Ye et al. 1999). Based on the construction of infectious cDNA clones of WYMV and CWMV (Yang et al. 2016; Zhang et al. 2021), the functions of several CWMV- and WYMV-encoded proteins have been characterized. For example, the coat protein (CP) of WYMV is associated with nucleocytoplasmic shuttling of genome-linked viral protein (VPg), possibly by assisting VPg in attaining a proper conformation during WYMV infection (Sun et al. 2013b). CWMV- and WYMV-encoded proteins target a series of host proteins to improve viral infection. In WYMV, nuclear inclusion-a protease (NIa-Pro) interacts with the host light-induced protein (LIP) to facilitate viral infection by perturbing the abscisic acid pathway (Zhang et al. 2019). A recent study revealed that NIb interacts with *T. aestivum* m6A methyltransferase B (TaMTB) to upregulate the m^6A level of WYMV RNA1 and stabilize viral RNA, thus promoting viral infection (Zhang et al. 2022). In CWMV, cysteine-rich protein (CRP) is phosphorylated by SAPK7 and plays a key role in CWMV infection (Li et al. 2022). Moreover, the 3′-untranslated region (UTR) of CWMV genomic RNAs interacts with the host eukaryotic translation elongation factor (eEF1A) to promote CWMV replication and translation (Chen et al. 2021). Nevertheless, the function of WYMV- or CWMV-encoded proteins and the infection mechanism of WYMV or CWMV remain unknown.

In this study, we collected wheat samples from seven provinces in China and investigated the function of the natural variation of CP on WYMV and CWMV infection. Our results showed that the distribution of WYMV and CWMV in China has expanded, and that natural variations of CP from different WYMV isolates are involved in viral infection.

Results

Identification of WYMV or CWMV in wheat leaves from different areas in China

Wheat leaves with typical yellow mosaic virus symptoms from different areas were sampled and confirmed using RT-PCR. Our results showed that CWMV was identified in Langfang, Hebei Province, and WYMV was obtained from different areas, including Wuhu and Luan at Anhui Province, Junan and Luohe at Henan Province, Baoji at Shaanxi Province, Yangzhou and Xuzhou at Jiangsu Province, Ninghai at Zhejiang Province, and Yantai at Shandong Province in China (Fig. 1 and Additional file 1: Figure S1). Among them, WYMV was first isolated from wheat samples in Baoji, Wuhu, Ninghai, and Luohe, and CWMV was first isolated from wheat leaves in Langfang. Full-length sequences of CWMV and WYMV isolates were then obtained by RNA-sequencing, RT-PCR, and RACE assays (Additional file 1: Figure S2). CWMV and WYMV isolates were named according to the time and identification site. Amino acid sequences differences in the CP of WYMV and CWMV isolates were then analyzed. Among Xuzhou-2022, Luan-2022, Luohe-2022 Yantai-2022, Wuhu-2021, Junan-2021,

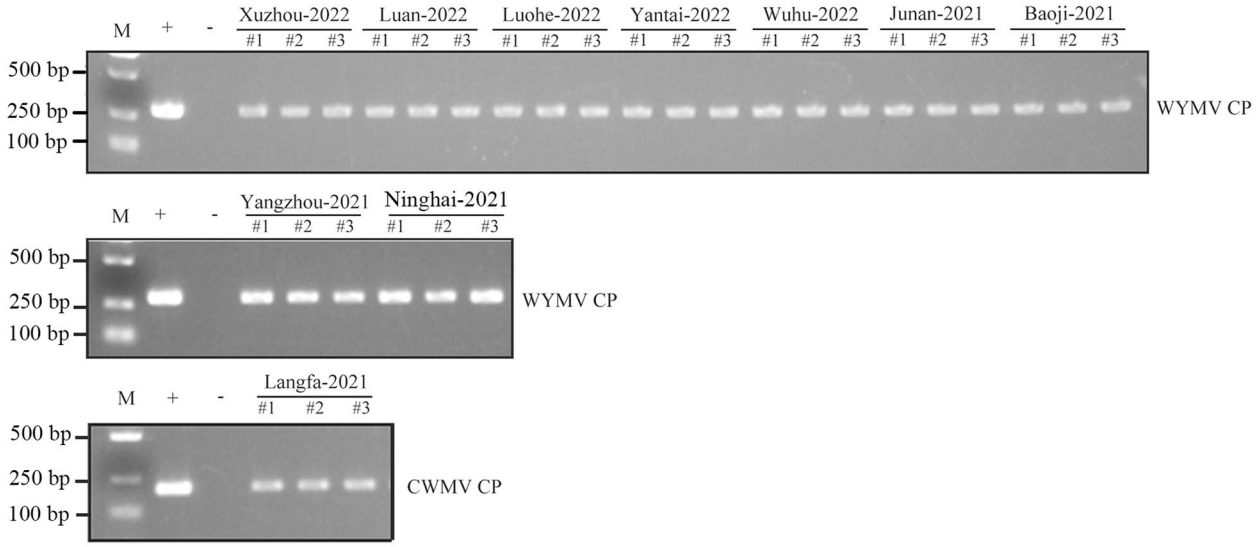

Fig. 1 Detection of CWMV and WYMV by RT-PCR in wheat samples collected from different areas in 2021 or 2022. The infectious clones and wheat leaves without viral infection was used as positive control (+) and negative control (-), respectively. M, DNA marker

Baoji-2021, Yangzhou-2021, and Ninghai-2021, the nucleotide identities of WYMV CP sequences were 98.94% to 100% (Additional file 1: Figure S3). Substitutions were observed at eight positions (103, 113, 116, 118, 119, 145, 160, and 178), locating in the N-terminal and middle region of CP (Table 1). Luan-2022 samples from Anhui Province, which had a unique amino acid substitution at position 160 (Ala to Ser), were observed in a previously characterized isolate (accession number AJ243984) from the same region. Furthermore, an amino acid substitution at position 116 (Ser to Ala) in Junan samples from Shandong Province was also observed in two previously characterized isolates (accession numbers AJ239039 and AJ240050). The CP of CWMV isolate Langfang-2021 are 530 nt in length and translating into 176 amino acid residues. The CP sequences of four CWMV isolates (Yantai-1999_1, Yantai-1999_2, Jiangsu-2006, and Rongcheng-2001, Additional file 2: Table S1) which had been submitted to NCBI database were used to do the sequence alignment with that of Langfang-2021. The results showed that 6, 1, 22, and 22 nucleotides in CP of Langfang-2021 was altered compared to that of Jiangsu-2006, Rongcheng-2001, Yantai-1999_1, and Yantai-1999_2, respectively. The CWMV CP sequences determined in this study had 95.86% to 100% (CP) nucleotide identity among Jiangsu-2006, Rongcheng-2001, Yantai-1999_1, and Yantai-1999_2. Three substitutions in CP amino acid at positions (12, 74, and 96) were identified (Table 2 and Additional file 1: Figure S4). Moreover, the CP amino acid of Langfang-2021 was same to that in Rongcheng-2003 (Additional file 1: Figure S4).

Table 1 Consensus amino acids at 7 positions in the wheat yellow mosaic virus coat protein amino acid sequence alignment for the virus isolates from various sampling areas in China

Position	Xuzhou-2022	Luan-2022	Luohe-2022	Yantai-2022	Wuhu-2021	Junan-2021	Baoji-2021	Yangzhou-2021	Ninghai-2021
103	D	D	D	D	D	N	D	N	N
113	I	V	I	V	V	I	V	I	I
116	N	D	N	D	D	D	D	N	N
118	S	S	S	S	S	A	S	S	S
119	I	I	I	V	I	I	I	I	I
145	I	I	I	I	I	T	I	T	I
160	A	S	A	A	A	A	A	A	A
178	A	A	A	A	V	V	V	V	V

Table 2 Consensus amino acids at 3 positions in the Chinese wheat mosaic virus coat protein amino acid sequence alignment for different CWMV isolates

Position	Langfang-2021	Jiangsu-2006	Rongcheng-2001	Yantai-1999_1	Yantai-1999_2
12	K	K	K	R	R
74	F	F	F	L	L
96	T	I	T	T	T

Phylogenetic analysis of CP from different WYMV isolates

A total of 90 WYMV CP sequences (9 from this study and 81 from previously published sequences from NCBI) were used for phylogenetic analysis. All CP sequences are 879 bp in length. The phylogenetic relationship of CP was analyzed using a nucleotide substitution model. The results showed that CP of Luan-2022 and Yantai-2022 clustered with those of previously reported corresponding isolates. Moreover, CP of WYMV isolates Baoji-2021, but not of Wuhu-2021, Ninghai-2021 Luohe-2022, and Xuzhou-2022, was clustered with those of previously reported isolates from the same province. However, CP of Junan-2021 and Yangzhou-2021 were not clustered with those of previously reported isolates from the same location (Fig. 2).

Natural variation of CP was involved in WYMV infection

Based on the results of the phylogenetic analysis, seven WYMV isolates (Wuhu-2021, Junan-2021, Baoji-2021, Yangzhou-2021, Ninghai-2021, Xuzhou-2022, and Luohe-2022) were not isolated previously and then were selected for further study. To analyze the function of the natural variation of CP in WYMV infection, we replaced the CP of WYMV infectious clones with that in these seven isolates to obtain recombinant plasmids (WYMV-WH-2021, WYMV-JN-2021, WYMV-BJ-2021, WYMV-YZ-2021, WYMV-NH-2021, WYMV-XZ-2022, and WYMV-LH-2022) (Fig. 3a). In vitro transcripts from linearized plasmids of pCB301-SP6-R1, WYMV-WH-2021, WYMV-JN-2021, WYMV-BJ-2021, WYMV-YZ-2021, WYMV-NH-2021, WYMV-XZ-2022, and WYMV-LH-2022 were respectively mixed with pCB301-SP6-R2, linearized and transcribed in vitro, to form 8 inocula (WYMV, WH-2021, JN-2021, BJ-2021, YZ-2021, NH-2021, XZ-2022, and LH-2022). Each inoculum was rubbed onto the leaves of the wheat cultivar Yangmai158 (YM158) and cultivated at 8°C, and pCB301-SP6-R1- and pCB301-SP6-R2-inoculated wheat plants were used as controls. At 7 days post-infiltration (dpi), the viral infection in wheat leaves was confirmed by RT-PCR assay using the CP specific primers (Additional file 1: Figure S5). The results of qRT-PCR and Western blot assay revealed that the accumulation level of WYMV RNA and CP at 28 dpi was significantly increased in the systemic leaves of WH-2021-, JN-2021-, YZ-2021-, NH-2021-, and LH-2022-inoculated plants compared to that in the pCB301-SP6-R1 + R2-inoculated control plants (Fig. 3b, c). In particular, the accumulation of WYMV RNA and protein at 28 dpi in YZ-2021- and LH-2022-inoculated wheat plants was increased by 15- and 4-fold compared than that in the control plants (Fig. 3b, c). In contrast, the accumulation of WYMV RNA and CP in plants infected with BJ-2021 and XZ-2021 did not change compared with that in plants inoculated with the original WYMV infectious clone (Fig. 3b, c). At 40 dpi, all the assayed wheat leaves showed typical viral symptoms. Consistant with the results of qRT-PCR, wheat leaves inoculated with WH-2021, JN-2021, YZ-2021, NH-2021, and LH-2022 showed much more mosaic and stunting symptoms than those inoculated with the control, whereas the viral symptoms in wheat leaves inoculated with BJ-2021 or XZ-2022 were similar to those in control plants (Fig. 3d).

Natural variation of CP from WYMV isolates Junan-2021 and Yangzhou-2021 enhanced WYMV infection in resistance cultivars

Homology analysis revealed that CP of Junan-2021 and Yangzhou-2021 isolates did not cluster with those of previously reported isolates from Junan and Yangzhou (Junan-old, accession number KX258947 and Yangzhou-2016, accession number AJ240051 and AJ131981) (Fig. 2). To analyze the functional difference of CP in WYMV isolates from the same region, we replaced the CP region of pCB301-SP6-R1 with CP in Junan-old and Yangzhou-2016 to produce the recombinant plasmids, WYMV-JN-old and WYMV-YZ-2016, respectively. After linearizing and transcribing in vitro, the in vitro transcription was mixed with pCB301-SP6-R2 linearized and transcribed in equal proportions to form two inocula (JN-old and YZ-2016). JN-old and JN-2021 were inoculated by rubbing the leaves of the main locally resistant wheat cultivars Lumai19 (LM19), Lumai23 (LM23), and Lumai14 (LM14) in Junan. Similarly, major local wheat cultivars Su553 (S553), Xuzhou (XZ14), and Sumai3 (SM3) in Yangzhou were infected with YZ-2016 and YZ-2021. At 7 dpi, we used to RT-PCR assay to confirm viral infection in wheat leaves (Additional file 1: Figure S6). The qRT-PCR and Western blot assay showed that the accumulation level of WYMV RNA and CP was significantly increased in systemic leaves of LM23 and decreased in that of LM14 inoculated with JN-2021 at 28 dpi, compared to those inoculated with JN-old (Fig. 4a and Additional file 1: Figure S7).

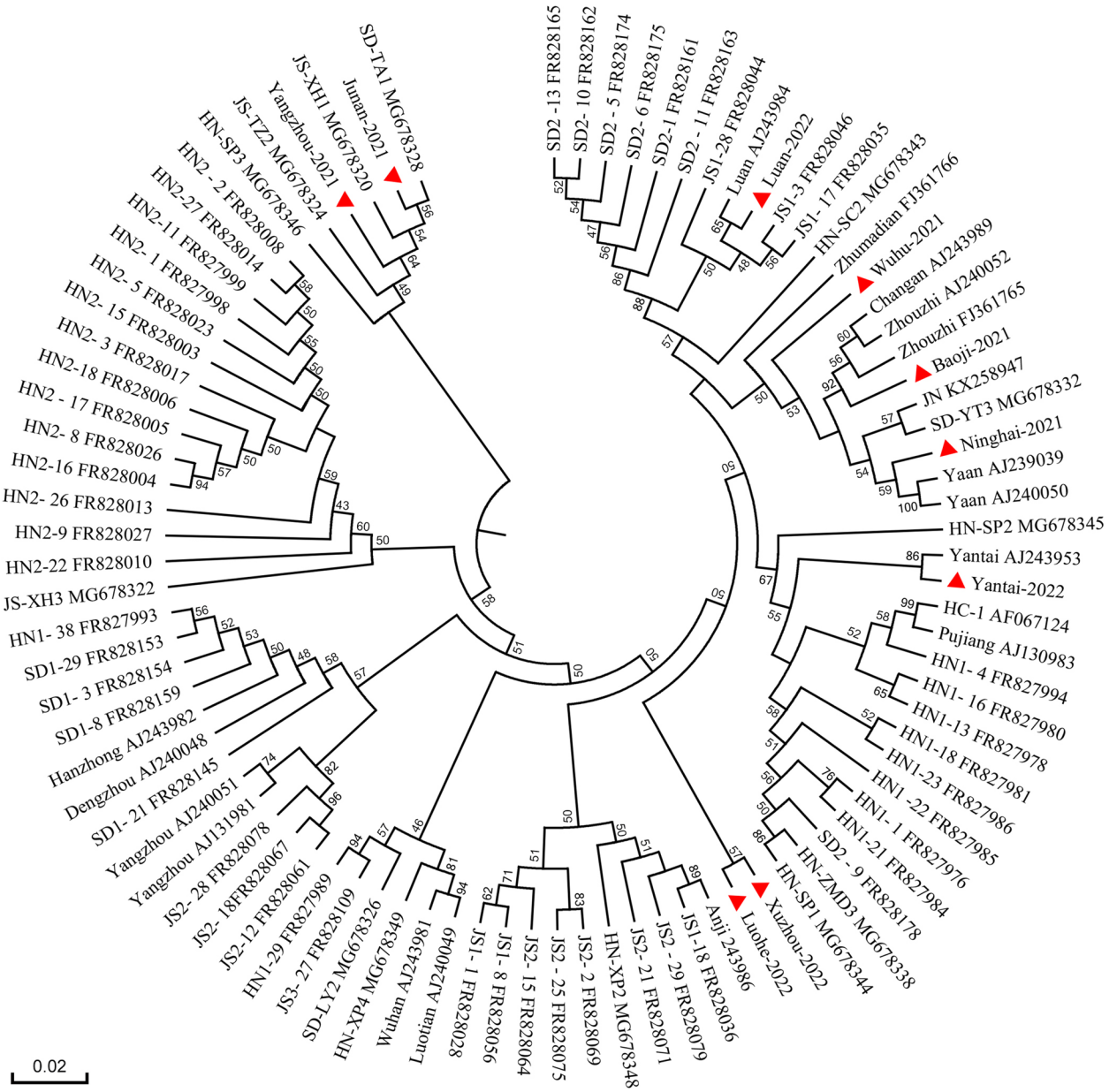

Fig. 2 Maximum likelihood phylogenetic analysis of 90 wheat yellow mosaic virus coat protein (CP)-encoding nucleotide sequences. Branches are labeled with the provenance of the sequence from this study and GenBank accession numbers. Sampling sites on the branches were represent for the location in China. Names of each of 9 isolates obtained in this study are preceded by a red triangle. Numbers at branches represent bootstrap values of 1000 replicates. Only bootstrap values ≥ 40% are shown

Moreover, the accumulation of WYMV RNA and CP in the systemic leaves of LM-19 plants infected with JN-2021 was similar to that in LM-19 plants infected with JN-old (Fig. 4a and Additional file 1: Figure S7). For resistance cultivars in Yangzhou, the accumulation of WYMV RNA and CP in the systemic leaves of YZ-2021-inoculated XZ-14 and SM3 plants were much higher than that in YZ-2016-inoculated XZ-14 and SM3 plants at 28 dpi. However, the accumulation of WYMV RNA and CP in the systemic leaves of S553 plants infected with YZ-2021 was much lower than that in plants infected with YZ-2016 (Fig. 4a and Additional file 1: Figure S7). At 40 dpi, the leaves of LM23, XZ-14, and SM3 inoculated with JN-2021 or YZ-2021 showed more mosaic and stunting symptoms than those inoculated with JN-old or YZ-2016. Mosaic

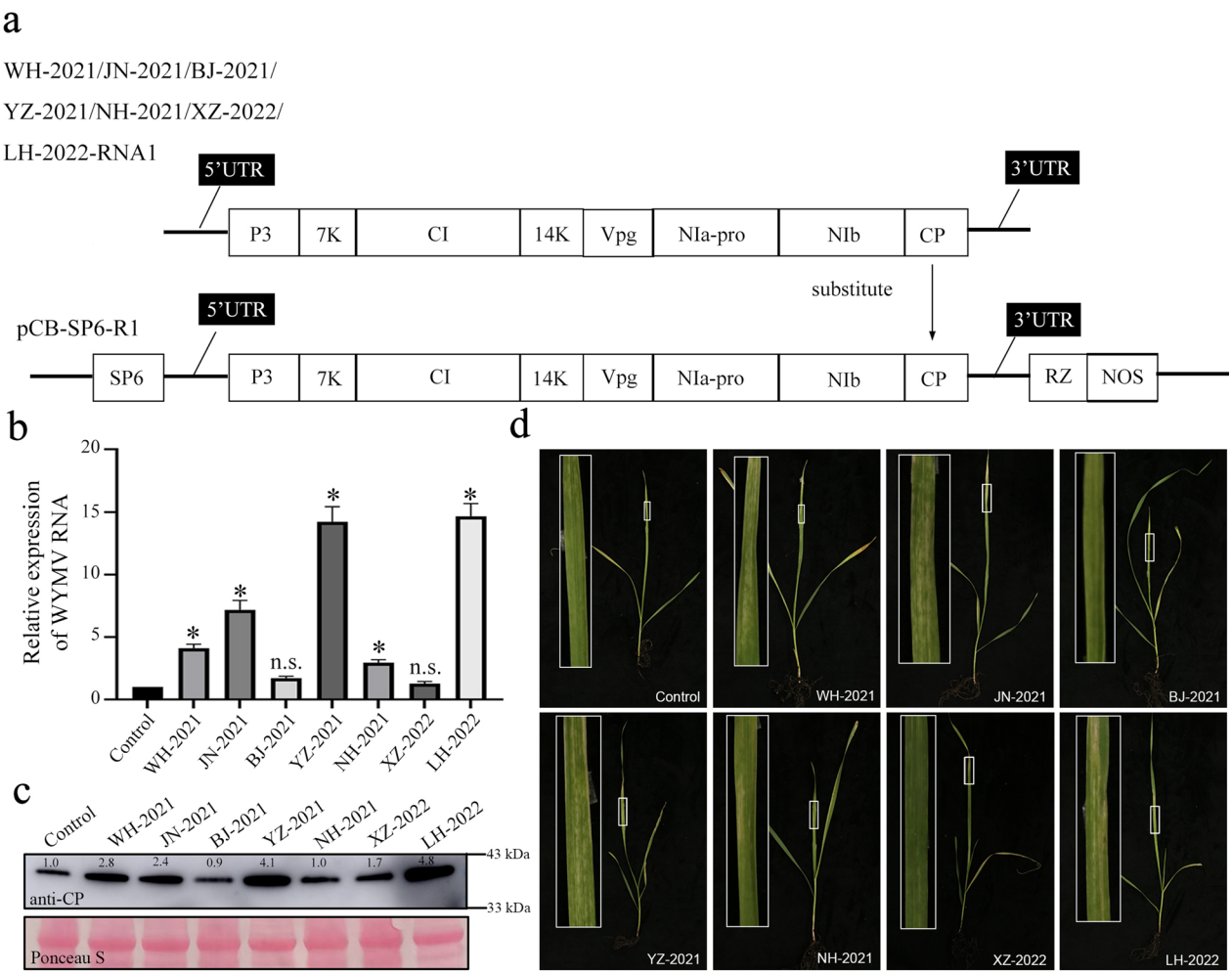

Fig. 3 Natural variation of coat protein (CP) from different WYMV isolates was involved in WYMV infection. **a** The schematic diagram of the infectious clones containing CP from different WYMV isolates (Wuhu-2021, Junan-2021, Baoji-2021, Yangzhou-2021, Ninghai-2021, Xuzhou-2022, and Luohe-2022). The CP on the previous WYMV infectious clone was replaced by the nucleotides of the CP sequence of different WYMV isolates obtained in this study. pCB-SP6-R1 represented of the WYMV infectious clone. **b** Relative expression of viral RNA in the systemic leaves of wheat plants inoculated with the infectious clones containing CP from different WYMV isolates at 28 days post-infiltration (dpi). Data shown are the means of three biological replicates ± the SE. The values were normalized to those for the reference gene (Cell Division Control protein, *TaCDC*) and are presented as fold changes in expression relative to that in control plants. Asterisks indicate significant differences in expression between wheat leaves inoculated with control and the infectious clones containing CP from different WYMV isolates when analyzed using a Student's *t*-test ($P < 0.05$). Control, wheat leaves inoculated with WYMV infectious clones which were constructed in previous study. **c** The systemic leaves of the wheat plant inoculated with the infectious clones containing CP from different WYMV isolates were harvested for testing the accumulation of viral protein by Western blot assay using CP specific antibody at 28 dpi. **d** The phenotype of wheat plants inoculated with the infectious clones containing CP of different WYMV isolates at 40 dpi

symptoms were not observed in the leaves of LM14 and S553 inoculated with JN-2021, YZ-2021, JN-old, and YZ-2016. The wheat leaves of LM-19 plants infected with JN-2021 showed viral symptoms similar to those of LM-19 plants infected with JN-old (Fig. 4b).

Functional analysis of natural variety of CP in CWMV infection

To analyze the function of the natural variety of CP of Langfang-2021 in CWMV infection, the CP sequence in CWMV infectious clone pCB301-CWMV-R2 was replaced with that of Langfang-2021, Jiangsu-2006, and Yantai-1999_1 (same to Yantai-1999_2) to obtain pCB301-CWMV-R2-LF-2021, pCB301-CWMV-R2-JS-2006, and pCB301-CWMV-R2-YT-1999, respectively. The inocula of LF-2021, JS-2006, and YT-1999 were obtained by mixing with pCB301-CWMV-R1 and pCB301-CWMV-R2-LF-2021, pCB301-CWMV-R2-JS-2006, or pCB301-CWMV-R2-YT-1999, and then inoculated individually into YM158. At 7 dpi, CWMV

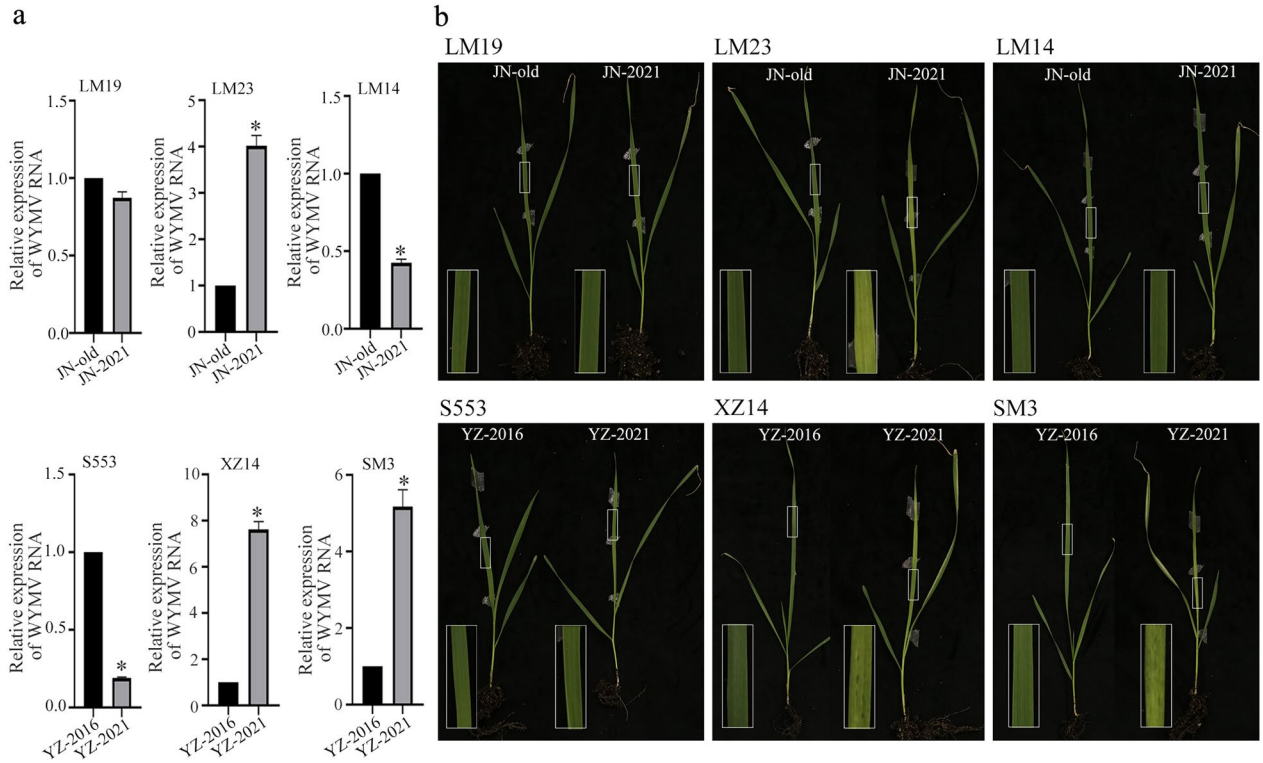

Fig. 4 Natural variation of coat protein (CP) from different WYMV isolates enhanced WYMV infection in several wheat resistance cultivars. **a** Relative expression of WYMV RNA in systemic leaves of wheat resistance cultivars inoculated with JN-old or JN-2021 and YZ-2016 or YZ-2021. LM 19, LM23, and LM14 are resistance cultivars in Junan. S553, XZ14, and SM3 are the resistance cultivars in Yangzhou at 28 days post-infiltration (dpi). JN-old and YZ-2016 represent for WYMV infectious clones containing CP from a previous WYMV isolate in Junnan and Yangzhou, China (Junan-old and Yangzhou-2016). JN-2021 and YZ-2021 represent for WYMV infectious clones containing CP from WYMV isolates Junan-2021 and Yang-2021 which obtained in this study. The values were normalized to those for the reference gene (*TaCDC*) and are presented as fold changes in expression relative to that in wheat leaves inoculated with JN-old or JN-2021 and YZ-2016 or YZ-2021. Asterisks indicate significant differences in expression between wheat leaves inoculated with JN-old and JN-2021 or YZ-2016 and YZ-2021 when analyzed using a Student's *t*-test ($P < 0.05$). **b** The phenotype of wheat plants inoculated with the infectious clones containing CP of WYMV isolate from Junnan and Yangzhou, China

RNA was detected in YM158 infected with LF-2021, JS-2006, or YT-1999 by RT-PCR assay (Additional file 1: Figure S8). At 28 dpi, the accumulation level of CWMV RNA, as well as CP protein, did not change in the systemic leaves of LF-2021- inoculated YM158 plants compared to that in JS-2006- or YT-1999-inoculated plant (Fig. 5a, b). Moreover, wheat plants inoculated with LF-2021, JS-2006, or YT-1999 showed mosaic symptoms similar to those inoculated with CWMV at 40 dpi (Fig. 5c). We also replaced the CP sequence in CWMV infectious clone 35S-CWMV-R2 with those in Langfang-2021, Jiangsu-2006, and Yantai-1999_1 to infect *Nicotiana benthamiana* plants. At 20 dpi, the accumulation of viral RNA and protein, as well as symptoms of systemic leaves, in the systemic leaves of *N. benthamiana* inoculated with LF-2021 were similar to those inoculated with JS-2006 or YT-1999 (Fig. 5d–f).

Discussion

A recent study showed that WYMV was mainly restricted to Shandong, Henan, Jiangsu, Anhui, Zhejiang, Hubei and Shaanxi provinces, and CWMV was identified in Hebei, Henan, and Shandong provinces (Yang et al. 2022). In this study, we confirmed that WYMV and CWMV-caused diseases in winter wheat were found in these provinces (Fig. 1 and Additional file 1: Figure S1). Although the WYMV isolates obtained from these areas were classified in different sub-groups according to the phylogenetic relationship of CP (Fig. 2), high protein sequence identity of CP in the assayed WYMV isolates was also identified (Table 1). These results indicate that the WYMV isolates from different areas are conserved. In addition, substitutions were observed at eight positions, in the N-terminal and middle regions of the CP (Table 1). Variations in the viral protein are shown to be involved in viral infection.

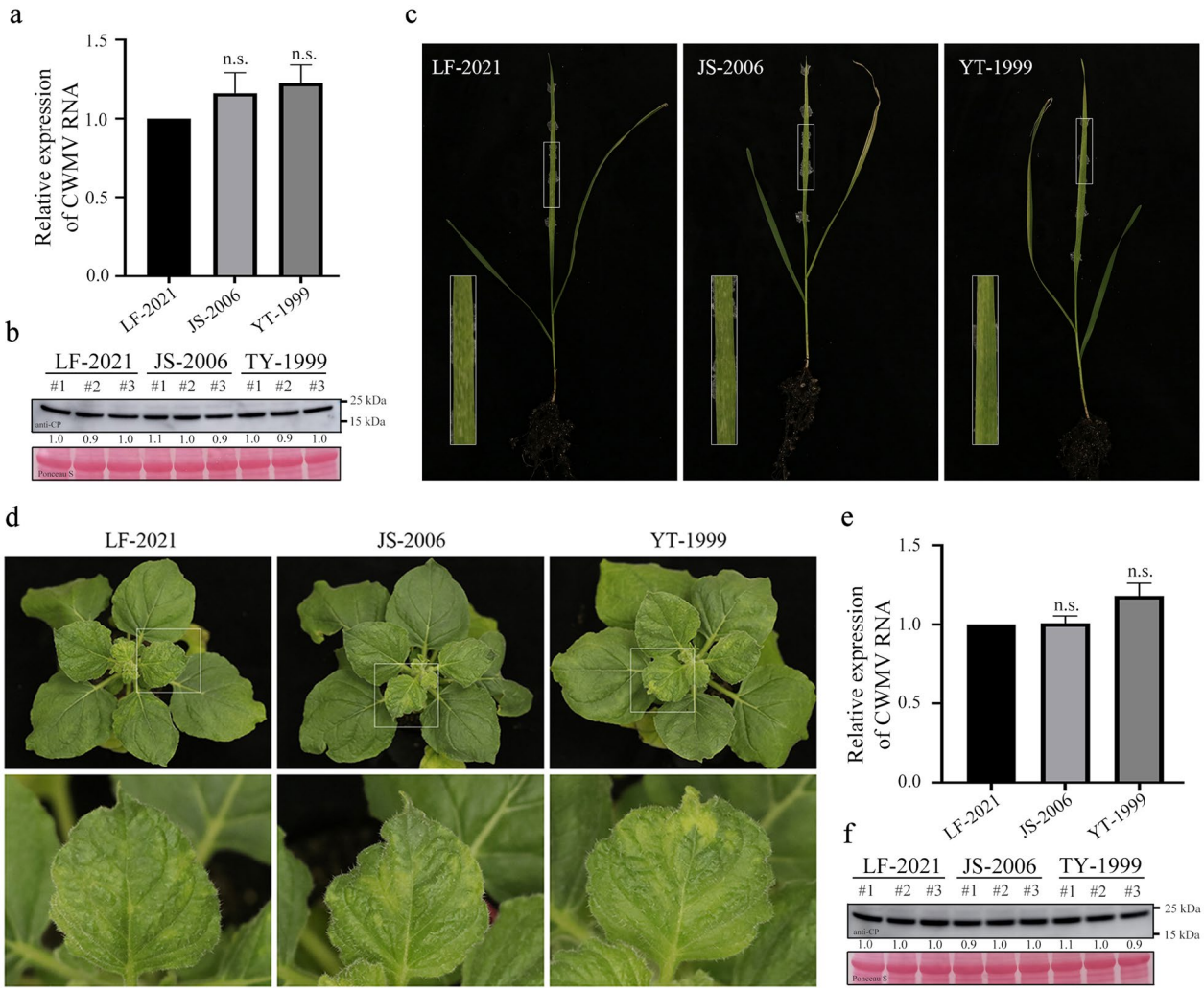

Fig. 5 The function of natural variation of coat protein (CP) from different CWMV isolates on CWMV infection. **a, b** The accumulation of CWMV RNA (**a**) and protein (**b**) in the systemic leaves of wheat plants inoculated with LF-2021, JS-2006, or YT-1999 at 28 dpi. LF-2021, JS-2006, and YT-1999 represent of the CWMV infectious clones containing CP from a previous isolate Langfang-2021, Jiangsu-2006, and Yantai-1999_1, respectively. The values were normalized to those for the reference gene (*TaCDC*) and are presented as fold changes in expression relative to that in wheat leaves inoculated with LF-2021, JS-2006, and YT-1999. Asterisks indicate significant differences in expression between wheat leaves inoculated with JS-2006 and LF-2021 when analyzed using a Student's *t*-test ($P < 0.05$). The CWMV protein accumulation was determined by estern blot using CP specific antibody. **c** The phenotype of wheat plants inoculated with JS-2006 and LF-2021 at 40 days post-infiltration (dpi). **d** Systemic mosaic symptoms in systemic leaves of *Nicotiana benthamiana* plants infected with JS-2006 and LF-2021 at 40 dpi. **e** Relative expression level of CWMV CP in the systemic leaves of *N. benthamiana* plants infected with LF-2021, JS-2006, and YT-1999. Values and error bars represent the mean ± SE of three independent biological replicates with three technical replicates per sample, *, $P < 0.05$ based on Student's *t*-test. **f** Western blot analysis of CWMV CP accumulation in the systemic leaves of *N. benthamiana* plants infected with LF-2021, JS-2006, and YT-1999 using CWMV CP specific antibody

For example, a previous study has shown that a potato virus Y (PVY) mutant strain, with single point mutations at two different nucleotide positions in the central part of the VPg, could overcome the resistance of Fva2 (a resistant tobacco line) (Lacroix et al. 2011). Our results also showed that the natural variation of CP was associated with WYMV infection (Fig. 3). Accordingly, the different infectivity among WYMV isolates obtained from different areas may be caused by those amino acid alterations.

Breeding resistant wheat varieties is the most feasible approach for controlling the disease (Chen et al. 2014). Previous studies have shown that WYMV resistance is controlled by 1–3 major genes (Liu et al. 2004). Moreover, 12 genes or quantitative trait loci (QTL), which play important roles in the resistance to WYMV infection, have been identified on chromosomes 2A, 2DL, 3BS, 5AL, 6DS, 7A, and 7BS (Yang et al. 2022). Although the

resistance genes in the wheat cultivars from Junan and Yangzhou used in this study were not identified, these cultivars did not show obvious viral symptoms after inoculation with the previous WYMV isolates. However, the wheat cultivars LM23 in Junan and XZ14 and SM3 in Yangzhou were susceptible to JN-2021 and YZ-2016, respectively (Fig. 4). Accumulating studies have shown that CP of post stranded RNA viruses plays multiple functions during plant-virus interactions (Weber and Bujarski 2015). On the one hand, CP could counteract plant antiviral defense. For example, during beet black scorch virus infection, CP subverts the MAPK signal-mediated antiviral innate immune response by targeting host factors (Gao et al. 2022). Thus, we propose that the variation in CP in field is likely to be involved in suppressing resistance mediated by resistance genes in the wheat cultivars LM23, XZ14, and SM3 and the wheat production was under threat as result of natural variation of CP in China. On the other hand, CP was also pivotal for pathogen-derived resistance in various crops (Prins et al. 2008; Gottula and Fuchs 2009). Such resistance may occur due to RNA silencing of the CP gene or directly interaction with host proteins (Weber and Bujarski 2015). In this study, viral RNA accumulation of JN-2021 and YZ-2021 was significantly reduced in LM14 and S553 compared to that of JN-old and YZ-2016 respectively (Fig. 4). Accordingly, we propose that the antiviral responses in wheat cultivars LM14 and S553 were activated by JN-2021 and YZ-2021 due to CP variation.

Pathogenic differences among wheat spindle streak mosaic virus isolates have been reported in China and Japan (Yang and Hou 2001; Kusume et al. 1997), which facilitated the identification of WYMV and provided further insights into the evolution of different isolates. The stability of CP in different WYMV isolates may present large discrepancies (Yang and Hou 2001). In addition to protecting the structure of the virus genome, potyviral CP is a multitasking protein that interferes with the majority of steps of the virus life cycle (Martínez-Turiño and García 2020). In this study, the pathogenicity of the WYMV mutants that replaced the CP region of different isolates varied significantly (Fig. 3), indicating that CP is involved in pathogenic variations in WYMV (Han et al. 2000). Sequence alignment of the CP of WYMV isolates (Wuhu-2021, Junan-2021, Baoji-2021, Yangzhou-2021, Ninghai-2021, Xuzhou-2022, and Luohe-2022) showed that eight positions were substituted (Table 1). Accordingly, we propose that one or more amino acids were modified among the WYMV isolates, resulting in pathogenicity differences. A recent study showed that N6-methyladenosine RNA modification in the CP region of WYMV RNA1 at the GGACA motif promotes WYMV genomic RNA stability and infection (Zhang et al. 2022). Sequence alignment indicated that the GGACA motif was altered among the WYMV isolates (Additional file 1: Figure S3), indicating that the pathogenicity difference of the WYMV isolates may be due to N6-methyladenosine RNA on RNA1. Protein function can be greatly modified by posttranslational modification (PTM) (Friso and van Wijk 2015), which may alter the pathogenicity of the virus in infected plants. For instance, SAPK7 phosphorylates CWMV CRP at S162 and S165 to promote CWMV infection in plants (Li et al. 2022). According to the amino acid comparison table for CP (Table 1), we found a substitution at positions 118 (Ser to Ala), suggesting that phosphorylation of Ser at these positions may be important for the pathogenicity of the WYMV isolate. However, further investigation is needed to elucidate the role of phosphorylation in the pathogenicity of WYMV isolates.

As mentioned earlier, WYMV and CWMV had been identified in wheat samples from several provinces in China (Han et al. 2000). In this study, we found that the distribution of WYMV and CWMV in growing areas in China has expanded in recent years. In addition, natural variations in CP from different WYMV isolates were associated with WYMV pathogenicity. Our results provided a theoretical basis for improving plant varieties to explain the rational distribution of disease-resistant varieties. To breed more effective resistant cultivars, the genetic mechanism of infection with different WYMV isolates needs to be clarified in the future.

Conclusions

In China, WYMV- and CWMV-induced yellow mosaic diseases seriously threaten the production of winter wheat (Yang et al. 2022). However, the genetic diversity of WYMV and CWMV in China has been largely unknown in recent years, making it difficult to control soil borne viral diseases in wheat. In this study, we randomly collected wheat samples from seven different regions of China and performed small RNA sequencing, RT-PCR, and RACE assays to confirm WYMV and CWMV infection. Compared with previous studies (Han et al. 2000), we found that the distribution of WYMV and CWMV tended to expand in recent years. Sequence alignment showed that some amino acid substitutions occurred in the CP of WYMV and CWMV from different wheat growing regions, which altered the pathogenicity of WYMV and CWMV. Notably, the infectious clones with the replaced CP from Junan and Yangzhou isolates enhanced WYMV infection in some local wheat-resistant varieties of Junan and Yangzhou. These results suggest that the natural variation in the WYMV genome is involved in its pathogenicity. However, the molecular mechanism remains to be further explored.

Methods

Plant materials

Wheat samples used in this study were obtained from different Chinese provinces, including Wuhu and Luan at Anhui Province, Junan and Luohe at Henan Province, Baoji at Shaanxi Province, Yangzhou and Xuzhou at Jiangsu Province, Ninghai at Zhejiang Province, Yantai at Shandong Province, and Langfang at Hebei Province, between March 2021 and April 2022. Leaves with typical yellow mosaic virus symptoms were examined using RT-PCR to confirm WYMV and CWMV infection. Leaf samples were collected from 10–20 randomly selected plants from each field and then stored at −80°C. Wheat (*T. aestivum*) cultivars Yangmai158 (YM158), Sumai3 (SM3), Xuzhou14 (XZ14), Su553 (S553), Lumai19 (LM19), Lumai23 (LM23), and Lumai14 (LM14) were inoculated with WYMV. Wheat and *N. benthamiana* leaves inoculated with WYMV/CWMV were frozen in liquid nitrogen and ground into fine powder for RNA and protein extraction.

Sequencing and rapid amplification of cDNA ends (RACE)

To obtain accurate and comprehensive information on WYMV and CWMV obtained from different areas in China, RNA sequencing and RT-PCR was performed to identify the sequences of WYMV and CWMV. Full length WYMV and CWMV isolates from different areas were obtained via RACE assay using the SMARTer® RACE 5′/3′ kit (Takara, Dalian, China) with Universal Primer A Mix (UPM) and sequence-specific primers following the manufacturer's instructions. The original data of RNA sequencing have been submitted to NCBI database (accession number PRJNA923775). Sequence-specific primers to determine the 5′-and 3′-terminal sequences are shown in Additional file 2: Table S2. Purified PCR products were ligated into the T-simple vector for sequencing.

Construction of infectious cDNA clones

The infectious full-length cDNA clones of WYMV (pCB301-SP6-R1/R2 for in vitro transcription) and CWMV (pCB301-CWMV-R1/R2 for in vitro transcription and 35S-CWMV-R1/R2 for *Agrobacterium* transformation) (Yang et al. 2016; Zhang et al. 2021) were used in this study. Overlap-PCR was performed to construct a plasmid with a full-length mutant WYMV RNA1 or CWMV RNA2. Briefly, CP was amplified from cDNA prepared from wheat leaf tissues infected with different WYMV or CWMV isolate using CP specific primers (Additional file 2: Table S2). PCR products from different WYMV isolates were substituted in the CP region of full-length infectious clone of pCB301-SP6-R1 (Zhang et al. 2021) to produce the infectious clones WYMV-XZ-2022, WYMV-LH-2022, WYMV-WH-2021, WYMV-JN-2021, WYMV-BJ-2021, WYMV-YZ-2021, WYMV-NH-2021, WYMV-JN-old, and WYMV-YZ-2016. Similarly, we obtained pCB301-R2-LF-2021 and pCB301-R2-JS-2006 by replacing the nucleotides in the CP sequence of the CWMV full-length infectious clone pCB301-R2.

In vitro transcription

pCB301-SP6-R1, WYMV-XZ-2022, WYMV-LH-2022, WYMV-WH-2021, WYMV-JN-2021, WYMV-BJ-2021, WYMV-YZ-2021, WYMV-NH-2021, WYMV-JN-old, WYMV-YZ-2016, and pCB301-SP6-R2 were linearized by performing *Spe*I restriction digestion and purified using repeated phenol/chloroform extraction and ethanol precipitation. Then, WYMV RNA1 and RNA2 linearized products were transcribed using the SP6 RNA synthesis kit (NEB, Beijing, China) in the presence of a cap analog (Promega, Fitchburg, WI, USA) according to the manufacturer's protocol. The RNA transcript products were electrophoresed on 1% agarose gels for quality and quantity assessments. Similarly, pCB301-CWMV-R1, pCB301-CWMV-R2, pCB301-CWMV-R2-LF-2021, and pCB301-CWMV-R2-JS-2006 plasmids were individually linearized with *Spe*I restriction enzyme, followed by in vitro transcription using the Ambion Message Machine kit (Invitrogen, Carlsbad, CA, USA).

Plant growth and virus inoculation

N. benthamiana and wheat cvs. YM158, SM3, XZ14, S553, LM19, LM23, and LM14 plants were grown in pots inside a greenhouse maintained at 25°C, 65 ± 5% relative humidity, and a 16 h light/8 h dark photoperiod. According to the previous studies (Yang et al. 2016; Zhang et al. 2021), the optimal temperature for CWMV replication is 15–17°C and 8°C was the most favorable temperature for the accumulation of WYMV. Thus, the plants inoculated with CWMV or WYMV were grown in a climate room maintained at 15°C or 8°C before further analysis, respectively. The CWMV infectious clones were individually transformed into *Agrobacterium tumefaciens* strain GV3101, and the *Agrobacterium* cultures were grown individually overnight in a yeast extract peptone medium (YEP) containing 50 mg/L of kanamycin and 50 mg/L of rifampicin at 28°C. The *Agrobacterium* cultures were centrifuged, and the pellets were suspended in an infiltration buffer (10 mM MES, 10 mM $MgCl_2$, and 100 μM acetosyringone) to a final OD_{600} concentration of 1.0, followed by incubation for 2 h. Mixed cultures (100 μL per leaf) were infiltrated individually into the whole second leaf of *N. benthamiana* plants (four weeks old) using needleless syringes. Wheat plants were grown to two-leaf stage in a greenhouse and then inoculated with in vitro transcripts of CWMV or WYMV after adding 1 vol of FES buffer (1%

wt/vol sodium pyrophosphate, 1% wt/vol macaloid, 1% wt/vol celite, 0.5 M glycine, 0.3 M K_2HPO_4, pH 8.5, with phosphoric acid). The mixture of RNA transcript products and FES was then inoculated into the second leaf of wheat (10 μL per leaf) by gently rubbing the surface with a gloved finger.

RNA extraction, RT-PCR, and qRT-PCR

Total RNA from wheat leaves (three leaves in each biological replicate) was extracted using the HiPure Plant RNA Mini Kit (Guangzhou Magen Biotechnology Co., China) following the manufacturer's instructions. First-strand cDNA synthesis was performed with 3 μg of RNA using the First Strand cDNA Synthesis kit (Toyobo, Kita-ku, Osaka, Japan) with random primers. PCR amplification was performed using a mixture containing 1 μL of template cDNA, following the protocol described in the Green Taq Mix DNA Polymerase (Vazyme, Nanjing, China). The cDNA was first denatured at 95°C for 5 min and then amplified by 35 cycles at 95°C for 30 s, 58°C for 20 s, and 72°C for 30 s, with a final incubation at 72°C for 10 min. After the reaction, PCR products were identified using 1% agarose gel electrophoresis. The above methods were also performed for the detection of wheat or *N. benthamiana* infected with WYMV and CWMV. The relative expression of WYMV and CWMV CP in wheat and *N. benthamiana* was confirmed using qRT-PCR with the SYBR Green qRT-PCR mixture and analyzed using the ABI7900HT Sequence Detection System (Applied Biosystems, Foster City, CA, USA). The relative expression levels of the assayed genes were calculated using the $2^{-\Delta\Delta CT}$ method. Each treatment had three biological replicates. The primers used for RT-PCR and qRT-PCR are listed in Additional file 2: Table S2.

Western blot assay

N. benthamiana tissue samples were frozen in liquid nitrogen, ground to a fine powder, and homogenized individually in a lysis buffer containing 60% SDS, 100 mM Tris–HCl (pH 8.8), and 2% β-mercaptoethanol for total protein extraction. Protein samples were separated via electrophoresis in 12% SDS-PAGE gels and then transferred onto nitrocellulose membranes. The membranes were incubated in blocking buffer (5% skim milk and 0.05% Tween 20 in 1 × TBS) for 60 min. Rabbit-derived specific primary antibodies and horseradish peroxidase-conjugated anti-rabbit secondary antibodies were used for detection. A chemiluminescence substrate was used to detect the protein signals.

Multiple sequence alignments

Nucleotide sequences were aligned using DNAMAN v.6.0 (Lynnon Biosoft Corp) and examined visually. Translation of nucleotide sequences into amino acid sequences and computation of percent nucleotide and amino acid identities between sequences were performed using DNAMAN.

Analysis of phylogenetic relationships

Phylogenetic trees based on CP were constructed using the maximum-likelihood (ML) method. A bootstrapped consensus tree was constructed from 500 replicates. Only the unique sequences (90 for CP) were considered for the phylogenetic analysis. All GenBank numbers of CP are listed in Additional file 2: Table S3. All phylogenetic analyses were performed using MEGA 6.0.

Statistical analysis

The Microsoft Excel software was used to calculate the mean values and standard errors of each experiment. The statistical software SPSS 16.0 was used to determine significant differences using *t*-test or Tukey's test. A significant difference with unequal variance between the two treatments was determined using a probability (*P*) value < 0.05.

Abbreviations

CDC	Cell division control protein
CI	N-terminal region of cylindrical inclusion protein
CP	Coat protein
CRP	Cysteine-rich protein
h	Hour
LIP	Light-induced protein
MES	4-Morpholineethanesulfonic acid
N. benthamiana	*Nicotiana benthamiana*
NIa-Pro	Nuclear inclusion-a protease
PCR	Polymerase chain reaction
P. graminis	*Polymyxa graminis*
PTM	Posttranslational modification
PVY	Potato virus Y
qRT-PCR	Quantitative reverse transcription-PCR
QTL	Quantitative trait loci
RACE	Rapid amplification of cDNA ends
RT-PCR	Reverse transcription-polymerase chain reaction
SAPK7	Serine/threonine-protein kinase
VPg	Viral protein genome-linked

Supplementary Information

The online version contains supplementary material available at https://doi.org/10.1186/s42483-023-00170-4.

Additional file 1: Figure S1. Detection of CWMV and WYMV by RT-PCR in wheat samples collected from different areas in 2021 or 2022 using coat protein (CP) specific primers. **Figure S2**. The full-length sequences of Xuzhou-2022, Luan-2022, Luohe-2022 Yantai-2022, Wuhu-2021, Junan-2021, Baoji-2021, Yangzhou-2021, Ninghai-2021, and Langfang-22021. **Figure S3**. Multiple sequence alignments of nucleotide and amino acid of coat protein (CP) from WYMV isolates from different area in China. **Figure S4**. Multiple sequence alignments of nucleotide and amino acid of coat protein (CP) from different CWMV isolates. **Figure S5**. Detection of WYMV by RT-PCR in wheat leaves inoculated with the infectious clones containing coat protein (CP) from seven WYMV isolates, including Wuhu-2021, Junan-2021, Baoji-2021, Yangzhou-2021, Ninghai-2021, Xuzhou-2022, and

Luohe-2022. **Figure S6**. Detection of WYMV by RT-PCR in the inoculated leaves of wheat resistance cultivars after infection with JN-old or JN-2021 and YZ-2016 or YZ-2021 at 7 days post-infiltration (dpi). **Figure S7**. The accumulation of WYMV protein in systemic leaves of wheat resistance cultivars inoculated with JN-old or JN-2021 and YZ-2016 or YZ-2021 at 28 days post-infiltration (dpi). **Figure S8**. Detection of CWMV by RT-PCR in the inoculated leaves of wheat or Nicotiana benthamiana plants after infection with LF-2021, JS-2006, or YT-1999 at 7 days post-infiltration (dpi).

Additional file 2: Table S1. The list of four CWMV isolates from China that had been submitted to NCBI database. **Table S2**. The primers used in this study. **Table S3.** The list of GeneBank Number used in phylogenetic tree.

Acknowledgements
Not applicable.

Authors' contributions
JL, JC, JY, and PL designed experiments. ZY and KZ performed the experiments of nucleotide sequences alignment. SL, ZC, HL, JZ, and QL performed the experiments of WYMV and CWMV identification. JL, JY, and PL wrote the manuscript. All authors read and approved the final manuscript.

Funding
This study was supported by the Science & Technology Public Welfare Project of Ningbo City, China (202002N3004), the Agriculture Research System from the Ministry of Agriculture of the P. R. China (CARS-03), and the National Natural Science Foundation of China (32100126).

Availability of data and materials
Not applicable.

Declarations

Ethics approval and consent to participate
Not applicable.

Consent for publication
Not applicable.

Competing interests
The authors declare that they have no competing interests.

Received: 30 November 2022 Accepted: 22 February 2023
Published online: 18 April 2023

References

Adams MJ. Epidemiology of fungally-transmitted viruses. Soil Use Manag. 2007;6:184–8. https://doi.org/10.1111/j.1475-2743.1990.tb00833.x.
Chen J. Occurrence of fungally transmitted wheat mosaic viruses in China. Ann Appl Biol. 2010;123:55–61. https://doi.org/10.1111/j.1744-7348.1993.tb04072.x.
Chen M, Sun L, Wu H, Chen J, Ma Y, Zhang X, et al. Durable field resistance to wheat yellow mosaic virus in transgenic wheat containing the antisense virus polymerase gene. Plant Biotechnol J. 2014;12:447–56. https://doi.org/10.1111/pbi.12151.
Chen X, He L, Xu M, Yang J, Li J, Zhang T, et al. Binding between elongation factor 1A and the 3′-UTR of Chinese wheat mosaic virus is crucial for virus infection. Mol Plant Pathol. 2021;22:1383–98. https://doi.org/10.1111/mpp.13120.
Chung BY, Miller WA, Atkins JF, Firth AE. An overlapping essential gene in the *Potyviridae*. Proc Natl Acad Sci. 2008;105:5897–902. https://doi.org/10.1073/pnas.0800468105.
Diao A, Chen J, Ye R, Zheng T, Yu S, Antoniw JF, et al. Complete sequence and genome properties of Chinese wheat mosaic virus, a new furovirus from China. J Gen Virol. 1999;80:1141–5. https://doi.org/10.1099/0022-1317-80-5-1141.
Friso G, van Wijk KJ. Posttranslational protein modifications in plant metabolism. Plant Physiol. 2015;169:1469–87. https://doi.org/10.1104/pp.15.01378.
Gao Z, Zhang D, Wang X, Zhang X, Wen Z, Zhang Q, et al. Coat proteins of necroviruses target 14-3-3a to subvert MAPKKKα-mediated antiviral immunity in plants. Nat Commun. 2022;13:716. https://doi.org/10.1038/s41467-022-28395-5.
Gottula J, Fuchs M. Toward a quarter century of pathogen-derived resistance and practical approaches to plant virus disease control. Adv Virus Res. 2009;75:161–83. https://doi.org/10.1016/S0065-3527(09)07505-8.
Han C, Li D, Xing Y, Zhu K, Tian Z, Cai Z, et al. wheat yellow mosaic virus widely occurring in Wheat (*Triticum aestivum*) in China. Plant Dis. 2000;84:627–30. https://doi.org/10.1094/PDIS.2000.84.6.627.
Kanyuka K, Ward E, Adams MJ. *Polymyxa graminis* and the cereal viruses it transmits: a research challenge. Mol Plant Pathol. 2003;4:393–406. https://doi.org/10.1046/j.1364-3703.2003.00177.x.
Kusume T, Tamada T, Hattori H, Tsuchiya T, Kubo K, Abe H, et al. Identification of a new wheat yellow mosaic virus strain with specific pathogenicity towards major wheat cultivars grown in Hokkaido. J J Phytopath. 1997;63:107–9. https://doi.org/10.3186/jjphytopath.63.107.
Lacroix C, Glais L, Verrier J-L, Jacquot E. Effect of passage of a *Potato virus Y* isolate on a line of tobacco containing the recessive resistance gene va^2 on the development of isolates capable of overcoming alleles 0 and 2. Eur J Plant Pathol. 2011;130:259–69. https://doi.org/10.1007/s10658-011-9751-0.
Li J, Feng H, Liu S, Liu P, Chen X, Yang J, et al. Phosphorylated viral protein evades plant immunity through interfering the function of RNA-binding protein. PLoS Pathog. 2022;18:e1010412. https://doi.org/10.1371/journal.ppat.1010412.
Liu W, He Z, Geng B, Hou M, Zhang M, Nie H, et al. Identification of resistance to yellow mosaic disease of wheat and analysis for its inheritance of some varieties. Acta Phytopathol Sin. 2004;34:542–7. https://doi.org/10.1300/J064v24n01_09.
Martínez-Turiño S, García JA. Potyviral coat protein and genomic RNA: a striking partnership leading virion assembly and more. Adv Virus Res. 2020;108:165–211. https://doi.org/10.1016/bs.aivir.2020.09.001.
McKinney HH. Investigations on the rosette disease of wheat and its control. J Agric Res. 1923;23:771–800.
Ohki T, Netsu O, Kojima H, Sakai J, Onuki M, Maoka T, et al. Biological and genetic diversity of *wheat yellow mosaic virus* (genus *Bymovirus*). Phytopathology. 2014;104:313–9. https://doi.org/10.1094/PHYTO-06-13-0150-R.
Ohki T, Sasaya T, Maoka T. Cylindrical inclusion protein of wheat yellow mosaic virus is involved in differential infection of wheat cultivars. Phytopathology. 2019;109:1475–80. https://doi.org/10.1094/PHYTO-11-18-0438-R.
Prins M, Laimer M, Noris E, Schubert J, Wassenegger M, Tepfer M. Strategies for antiviral resistance in transgenic plants. Mol Plant Pathol. 2008;9:73–83. https://doi.org/10.1111/j.1364-3703.2007.00447.x.
Sawada E. Control of wheat yellow mosaic virus. J Plant Prot. 1972;14:444.
Shirako Y, Suzuki N, French RC. Similarity and divergence among viruses in the genus *Furovirus*. Virology. 2000;270:201–7. https://doi.org/10.1006/viro.2000.0251.
Sohn A, Schenk P, Signoret PA, Schmitz G, Schell J, Steinbiss HH. Sequence analysis of the 3′-terminal half of RNA 1 of wheat spindle streak mosaic virus. Arch Virol. 1994;135:279–92. https://doi.org/10.1007/bf01310014.
Sun BJ, Sun LY, Tugume AK, Adams MJ, Yang J, Xie LH, et al. Selection pressure and founder effects constrain genetic variation in differentiated populations of soilborne bymovirus wheat yellow mosaic virus (*Potyviridae*) in China. Phytopathology. 2013a;103:949–59. https://doi.org/10.1094/PHYTO-01-13-0013-R.
Sun L, Jing B, Andika IB, Hu Y, Sun B, Xiang R, et al. Nucleo-cytoplasmic shuttling of VPg encoded by wheat yellow mosaic virus requires association with the coat protein. J Gen Virol. 2013b;94:2790–802. https://doi.org/10.1099/vir.0.055830-0.
Weber PH, Bujarski JJ. Multiple functions of capsid proteins in (+) stranded RNA viruses during plant-virus interactions. Virus Res. 2015;196:140–9. https://doi.org/10.1016/j.virusres.2014.11.014.
Yang J, Hou MS. Identification of the partial sequence of pathogen responsible for wheat mosaic disease in Hubei Province. Acta Phytopathol Sin. 2001;31(4):319–23. https://doi.org/10.3321/j.issn:0412-0914.2001.04.007.
Yang J, Zhang F, Xie L, Song XJ, Li J, Chen JP, et al. Functional identification of two minor capsid proteins from Chinese wheat mosaic virus using its

infectious full-length cDNA clones. J Gen Virol. 2016;97:2441–50. https://doi.org/10.1099/jgv.0.000532.
Yang J, Liu P, Zhong K, Ge T, Chen L, Hu H, et al. Advances in understanding the soil-borne viruses of wheat: from the laboratory bench to strategies for disease control in the field. Phytopathol Res. 2022;4:27. https://doi.org/10.1186/s42483-022-00132-2.
Ye R, Zheng T, Chen J, Diao A, Adams MJ, Yu S, et al. Characterization and partial sequence of a new furovirus of wheat in China. Plant Pathol. 1999;48:379–87. https://doi.org/10.1046/j.1365-3059.1999.00358.x.
Zhang T, Liu P, Zhong K, Zhang F, Xu M, He L, et al. Wheat yellow mosaic virus NIb interacting with host light induced protein (LIP) facilitates its infection through perturbing the abscisic acid pathway in wheat. Biology. 2019;8:80. https://doi.org/10.3390/biology8040080.
Zhang F, Liu S, Zhang T, Ye Z, Han X, Zhong K, et al. Construction and biological characterization of an infectious full-length cDNA clone of a Chinese isolate of wheat yellow mosaic virus. Virology. 2021;556:101–9. https://doi.org/10.1016/j.virol.2021.01.018.
Zhang T, Shi C, Hu H, Zhang Z, Wang Z, Chen Z, et al. N6-methyladenosine RNA modification promotes viral genomic RNA stability and infection. Nat Commun. 2022;13:6576. https://doi.org/10.1038/s41467-022-34362-x.